X-RAY AND OPTICAL OBSERVATIONS OF THE STAR FORMING REGION NGC 2264

E. FLACCOMIO[1], S. SCIORTINO[1], G. MICELA[1], F. DAMIANI[1], F. FAVATA[2], C. CORBALLY[3], A. TOMANEY[3], F.R. HARNDEN JR.[4], J. SCHACHTER[4]

[1] *Istituto e Osservatorio Astronomico di Palermo, Palermo, Italy*

[2] *European Space Agency, Astrophysics Division, ESTEC*

[3] *Vatican Observatory*

[4] *Harvard-Smithsonian Center for Astrophysics, Cambridge (MA), U.S.A.*

ABSTRACT. We present a ROSAT High Resolution Imager (HRI) observation of the star forming region NGC 2264. The analysis has detected more than 40 X-ray sources with L_x in the range $10^{30} - 10^{31}$ erg/sec. The high spatial resolution of the detector allows us to resolve sources that were confused in previous IPC and PSPC observations of the same region.

Moreover, we have performed CCD photometric observations in the BVRI bands of the Johnson-Cousin system at the Vatican Advanced Technology Telescope (VATT) of the central region of the HRI field of view were the spatial concentration of X-ray sources is highest. We have obtained photometry for 530 stars with $V \leq 22$. From the X-ray properties and the photometry we have selected ~ 150 stars as possible association members. We discuss the implications of our results on the Initial Mass Function.

1. Introduction

Placed at about 950 pc (Pérez et al., 1987), the star forming region (SFR) NGC2264, is more distant than other well studied regions with similar characteristics (e.g. Taurus-Auriga or Orion Trapezium). Still it offers a good opportunity of enriching our knowledge of the processes involved in the first stages of star evolution.

In fact, the interpretation of the observational data is greatly eased by two factors: a small *interstellar* visual absorption ($\mathrm{E(B-V)} = 0.06$ mag.; Pérez et al., 1987) for the cluster members and the presence, in the immediate proximity of the region, of an optically thick cloud that effectively obscures background stars.

2. The observations

We have obtained 1 HRI pointing, with exposure time of 10 ksec, and BVRI CCD imaging on a subregion of about 20 x 20 arcmin toward NGC2264. The X-ray data were analyzed with the Damiani et al. (1997) detection and photometry algorithm based on wavelet transforms. 43 resolved sources were detected with count rates in the 0.89-6.29 cts/ksec range. Assuming all the sources at the distance of 950 pc and a conversion factor for a single temperature plasma emission with kT = 1.0 keV and interstellar medium with log $N_H = 20.7$ we calculated the X-ray luminosities ($29.98 \leq \log\ L_X \leq 30.83$).

Errors on the X-ray luminosities, calculated allowing for uncertainties on the statistic and spectrum, are in the 30-100% range with a median value of 50%.

The optical observations were performed at the 1.8m Vatican Advanced Technology Telescope (VATT), on Mt. Graham (Arizona). We obtained (B,V,R_c,I_c) photometry for 530 stars, of which 134 brighter than the magnitude limit of standard stars ($V \lesssim 16$). Photometric uncertainties, as given by the residuals of the standard star transformation, are smaller than 0.05 magnitudes in all bands.

3. The color-color diagrams and the selection of NGC2264 members

The NGC2264 color-color diagrams show that most of the redder objects deviate from both the main sequence (MS) and the giant loci. These deviations are most likely due to blue excesses in the spectra of these objects rather than to interstellar reddening. This suggests that they are T Tauri stars for which rather large blue excesses have been quite successfully related to the presence of a boundary layer between the star and the surrounding accretion disk (e.g. Bertout et al. 1988).

Indeed, the stars in our region whose Hα line was detected in emission by Herbig (1954), Marcy (1989) and Ogura (1984) show, on average, larger blue excesses than the X-ray sources: while the former are mostly CTTS, the latter are, more likely, WTTS with less or no blue excess. It is then clear that the distance from the locus of pure photospheric emission can be interpreted as an indicator of disk activity and, consequently, of membership to the SFR.

In the R-I vs. V-R diagram the main and giant sequences are nearly coincident. Hence, any PMS star should have intrinsic "photospheric" colors falling in the narrow region between the two loci. A star that is significantly above the MS (i.e. by more than the photometric errors), is very likely affected by an excess in the V band on non-stellar origin, indicating its PMS nature. On the other hand the presence of a few stars below and to the right of the MS can be explained assuming a larger than average reddening. As the cloud right behind NGC2264 can be considered *totally* opaque, the most plausible possibility is that these object are NGC2264 members either with a high *circumstellar* absorption or partially embedded in the cloud.

Our NGC2264 member catalog, listing 149 members, is thus made up by: all the stars having colors significantly different from MS ones, the stars detected in X-rays in our HRI observation, the stars with Hα emission from the catalogs of Herbig (1954), Marcy (1989) and Ogura (1984), the stars from Vasilevskis et al. (1965) with proper motion membership probabilities greater than 50%.

4. The NGC2264 Mass Function

Figure 1 shows the HR diagram for the stars selected as NGC2264 members as described above together with the D'Antona & Mazzitelli (1994) evolutionary tracks. Bolometric luminosities and temperatures were derived from our photometric data using standard V-I vs. $T_{\rm eff}$ and V-I vs. BC_I relations. A correction for mean reddening was applied. However, individual differential reddening and color excess may introduce competing systematic shifts in the effective temperature and bolometric correction of each star.

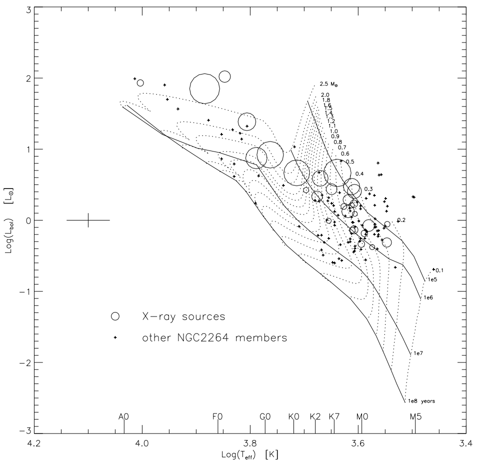

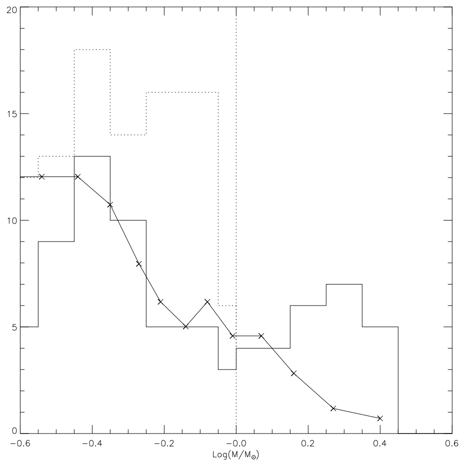

Fig. 1. [left] HR diagram of the X-ray sources and other NGC2264 members. Circle radii are proportional to the HRI luminosities of the stars detected in X-rays and unambiguously identified with optical sources. D'Antona & Mazzitelli (1994) evolutionary tracks and isochrones are shown. The cross indicates the typical uncertainties.

Fig. 2. [right] Our "best guess" IMF of NGC2264 (solid histogram). The dotted histogram includes the color-selected members and the line represents the Scalo (1986) IMF. The vertical line at $\log M/M_\odot = 0$ marks the division between the low and high mass ranges where, as explained in the text, the IMF was calculated differently.

In order to build a meaningful IMF it is important to take into account the completeness of the star samples used. Due to severe mass-dependent biases in the photometrically selected members, we have initially decided to exclude these stars for the calculation of the IMF.

Assuming that the fractions of NGC2264 members detected in X-rays and Hα are equal to the fractions of proper-motion stars detected in the same ways, we have estimated the completeness of the X-ray and Hα samples. The results show that, in the mass range $0.7 \leq M/M_\odot \leq 1.0$, the only one in which the samples overlap significantly, the X-ray and the Hα samples are individually incomplete but their union is indeed complete (within the statistical uncertainties). The union sample has been thus used to build the IMF for $M \leq 1.0 M_\odot$. For masses greater than 1.0 $M_\odot$ the Hα and X-ray selection criteria are known to result in serious incompleteness, so that we also used the proper motion sample, which should be reasonably complete for $M > 1.0 M_\odot$. The result is the solid line histogram shown in Fig. 2; the line represents the Scalo (1986) local IMF with arbitrary normalization. Note that the apparent lack of stars with $\log M/M_\odot \lesssim -0.4$ is probably an artifact due to the limited sensitivity of the observations.

The most striking feature of this IMF is probably the lack of stars at $\log M/M_\odot \sim 0$. It is important to note however that this feature *may* be a byproduct of the way the IMF was built, and that, in spite of our effort, not every biases may have been accounted for.

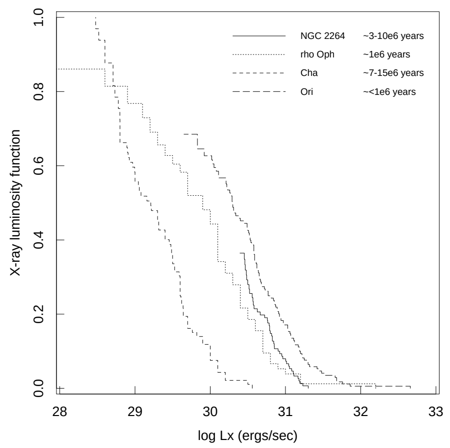

Fig. 3. Kaplan-Meier estimator for the NGC2264 X-ray luminosity function compared with those obtained for other SFRs by Casanova et al. (1995, ρ Ophiuchi), Feigelson et al. (1993, Chamaeleon I), Gagné et al. (1995, Orion).

As a matter of fact, if we had included the color-excess selected sample, we would have had a larger number of low mass members (dotted histogram in Fig. 2). This anyway contrasts with the presumed completeness of the X-ray + Hα samples in that mass range.

5. The X-ray luminosity function

Using both the X-ray luminosities for detected sources and upper limits on undetected NGC2264 possible members, we built the integrated luminosity function which is shown as a solid line in Fig. 3. The figure also shows, for comparison, the luminosity functions of three other SFRs of varying age, built from the data published in the paper of Casanova et al. (1995), Feigelson et al. (1993), Gagné et al. (1995). Note that the sequence of the luminosity functions from lower to higher X- ray luminosities suggests a dependence of activity from the age of the SFR, in agreement with previous results.

References

Bertout, C., Basri, G. & Bouvier, J. 1988, ApJ, 330, 350.
Casanova, S., Montmerle, T., Feigelson, E.D., André, P. 1995, ApJ, 439, 752.
D'Antona, F. & Mazzitelli, I. 1994, ApJS, 90, 476.
Damiani, F., Maggio, A., Micela, G., Sciortino, S. 1997, ApJ, 483, 350.
Feigelson, E.D., Casanova, S., Montmerle, T. & Guibert, J. 1993, ApJ, 416, 623.
Gagné, M., Caillault, J.P. & Stauffer, J.R. 1995, 445, 280.
Herbig, G.H., 1954, ApJ, 119, 483.
Marcy, G.W. 1989, AJ, 85, 230.
Ogura, K. 1984, P.A.S.J., 36, 139.
Pérez, M.R., Thé, P.S. & Westerlund, B.E. 1987, P.A.S.P., 99, 1050.
Vasilevskis, S., Sanders, W.L. & Balz, A.G.A.J. 1956, AJ, 70, 797.